

Is Your Explanation Reliable: Confidence-Aware Explanation on Graph Neural Networks

Jiaxing Zhang*

jz48@njit.com

New Jersey Institute of Technology
Newark, New Jersey, USA

Dongsheng Luo

dluo@fiu.edu

Florida International University
Miami, Florida, USA

Xiaoou Liu*

xiaoouli@asu.edu

Arizona State University
Tempe, Arizona, USA

Hua Wei[†]

hua.wei@asu.edu

Arizona State University
Tempe, Arizona, USA

Abstract

Explaining Graph Neural Networks (GNNs) has garnered significant attention due to the need for interpretability, enabling users to understand the behavior of these black-box models better and extract valuable insights from their predictions. While numerous post-hoc instance-level explanation methods have been proposed to interpret GNN predictions, the reliability of these explanations remains uncertain, particularly in the out-of-distribution or unknown test datasets. In this paper, we address this challenge by introducing an explainer framework with the confidence scoring module (ConfExplainer), grounded in theoretical principle, which is generalized graph information bottleneck with confidence constraint (GIB-CC), that quantifies the reliability of generated explanations. Experimental results demonstrate the superiority of our approach, highlighting the effectiveness of the confidence score in enhancing the trustworthiness and robustness of GNN explanations.

CCS Concepts

• **Human-centered computing** → *Human computer interaction (HCI)*; • **Computing methodologies** → **Neural networks**; *Artificial intelligence*.

Keywords

Graph Neural Network, Explainable AI, Confidence

ACM Reference Format:

Jiaxing Zhang, Xiaoou Liu, Dongsheng Luo, and Hua Wei. 2025. Is Your Explanation Reliable: Confidence-Aware Explanation on Graph Neural Networks. In *Proceedings of the 31st ACM SIGKDD Conference on Knowledge Discovery and Data Mining V.2 (KDD '25)*, August 3–7, 2025, Toronto, ON, Canada. ACM, New York, NY, USA, 12 pages. <https://doi.org/10.1145/3711896.3737010>

*Both authors contributed equally to this research.

[†]Corresponding author

Permission to make digital or hard copies of all or part of this work for personal or classroom use is granted without fee provided that copies are not made or distributed for profit or commercial advantage and that copies bear this notice and the full citation on the first page. Copyrights for components of this work owned by others than the author(s) must be honored. Abstracting with credit is permitted. To copy otherwise, or republish, to post on servers or to redistribute to lists, requires prior specific permission and/or a fee. Request permissions from permissions@acm.org.

KDD '25, August 3–7, 2025, Toronto, ON, Canada

© 2025 Copyright held by the owner/author(s). Publication rights licensed to ACM.

ACM ISBN 979-8-4007-1454-2/2025/08

<https://doi.org/10.1145/3711896.3737010>

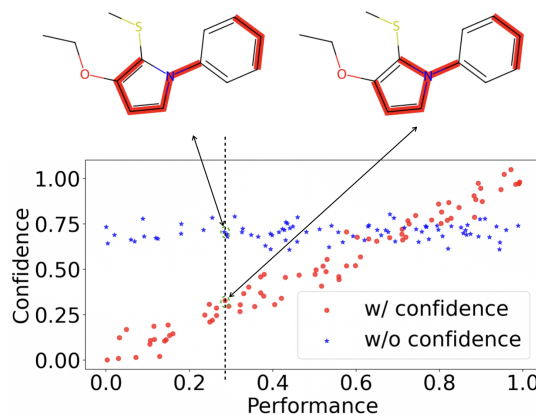


Figure 1: This figure illustrates the explanations and confidences generated by explainers with and without confidence-aware mechanism. The ground truth explanation in this case is the benzene ring; both samples have a low accuracy.

KDD Availability Link:

The source code of this paper has been made publicly available at <https://doi.org/10.5281/zenodo.15540314>.

1 Introduction

Graph Neural Networks (GNNs) have emerged as powerful tools for learning from graph-structured data, with applications spanning recommendation systems [11, 19], molecular chemistry [24, 30], traffic prediction [15, 26, 29, 32], and social network analysis [39]. Despite their impressive predictive capabilities, GNNs lack transparency, making it challenging to understand their decision-making process. This opacity is particularly concerning in high-stakes applications such as healthcare, finance, and scientific discovery, where understanding model predictions is as critical as the predictions themselves [1]. Consequently, there is a growing interest in explainability methods that aim to elucidate how GNNs arrive at specific predictions [9]. A prominent direction for post-hoc explainability in GNNs involves identifying critical substructures (i.e., nodes and edges) that most influence the model's decisions. Methods such as GNNExplainer[31] and PGExplainer[17] generate explanations by masking or perturbing parts of the input graph to determine which

components are most influential. More recently, Graph Information Bottleneck (GIB)-based methods [7, 18, 28, 33] have provided a principled framework for explainability, aiming to maximize mutual information between the explanation and the target output while compressing redundant information. The Information Bottleneck (IB) principle has demonstrated significant potential in balancing between representation relevance and compression, making it a robust theoretical foundation for explainable GNNs.

However, existing GIB-based methods and other post-hoc explainability techniques largely overlook an essential aspect—the confidence of the explanation itself. While these methods generate explanations, they do not quantify how reliable or trustworthy those explanations are [25]. This limitation is particularly concerning when models are deployed in out-of-distribution (OOD) or unknown test set scenarios, where explanations may degrade unpredictably. An explanation with high confidence but poor fidelity can be misleading [10], potentially leading to incorrect human interpretations in critical decision-making settings (e.g., medical diagnosis or financial risk assessment [16, 38]).

We hypothesize that the confidence of an explainer should align with its performance. If an explainer produces unreliable explanations, it should reflect low confidence, rather than misleadingly indicating high certainty. Conversely, high-quality explanations should be accompanied by high confidence scores. However, existing explainability methods do not provide such confidence quantification, leading to potential mismatches between explanation quality and user trust. As illustrated in Figure 1, the confidences of explanations generated by non-confidence-aware explainers (blue points) fail to distinguish between high- and low-fidelity explanations, whereas our confidence-aware approach (red points) provides well-calibrated confidence scores that align with the true reliability of the explanation. This highlights the necessity of confidence-aware explanation mechanisms in GNNs.

To address this limitation, we propose a Generalized Graph Information Bottleneck with Confidence Constraints (GIB-CC), an extension of GIB that explicitly integrates confidence estimation into the explanation generation process and a confidence-aware explainer framework accordingly. We conduct extensive experiments to evaluate the effectiveness of our confidence evaluation module. Our results demonstrate that incorporating confidence scores not only improves the performance of GNN explainers but also provides valuable insights into the reliability of their explanations. This advancement holds significant promise for deploying GNNs in critical applications where understanding model decisions is as important as the decisions themselves. In summary, this work aims to bridge the gap between interpretability and reliability in GNN explanations, targeting critical challenges in applying GNNs to real-world scenarios. Our approach aligns with the growing demand for trustworthy AI, where understanding not only what a model predicts but also how confident it is in its explanations is essential for responsible decision-making. Our key contributions include:

1. **Confidence-Aware Explainer (ConfExplainer)**, where we introduce an explainer with confidence scoring model that dynamically assesses the reliability of graph-level explanations. This enables users to gauge whether an explanation can be trusted or should be interpreted with caution.

2. **Confidence-Guided Information Bottleneck Objective**: We extend the GIB framework by incorporating confidence constraints (GIB-CC), allowing our framework to adaptively weigh explanations based on their reliability. This approach effectively reduces uncertainty and enhances the robustness of the explanations, particularly in OOD or unknown test set scenarios.

3. **Empirical Validation on Diverse Datasets**: We conduct comprehensive experiments on multiple benchmark datasets, including synthetic and molecular graphs, demonstrating our framework’s performance in both explanation fidelity and confidence calibration.

2 Related Work

GNN Explanation. Many attempts have been made to interpret GNN models and explain their predictions [17, 22, 23, 27, 31, 34]. These methods can be grouped into two categories based on granularity: (1) instance-level explanation, which explains the prediction for each instance by identifying significant substructures [22, 31, 34, 36], and (2) model-level explanation, which seeks to understand the global decision rules captured by the GNN [4, 17, 23]. From a methodological perspective, existing methods can be classified as (1) self-explainable GNNs [4, 8], where the GNN can provide both predictions and explanations and (2) post-hoc explanations [17, 31, 34], which use another model or strategy to explain the target GNN. In this work, we focus on post-hoc instance-level explanations, which involve identifying instance-wise critical substructures to explain the prediction. Various strategies have been explored, including gradient signals, perturbed predictions, and decomposition.

Perturbed prediction-based methods are the most widely used in post-hoc instance-level explanations. The idea is to learn a perturbation mask that filters out non-important connections (label irrelevant) and identifies dominant substructures (label preserving) while preserving the original predictions. For example, GNNExplainer [31] uses end-to-end learned soft masks on node attributes and graph structures, while PGExplainer [17] incorporates a graph weight generator to incorporate global information. RGExplainer [22] uses reinforcement learning technology with starting point selection to find important substructures for the explanation.

Confidence Estimation. However, existing GIB-based methods lack confidence estimation, which is essential for distinguishing between reliable and misleading explanations, particularly under distribution shifts. Although techniques such as Monte Carlo Dropout and Deep Ensembles [25] have been applied to uncertainty estimation in GNNs, they focus on predictive confidence rather than explanation confidence, leaving a gap in quantifying the trustworthiness of explanations themselves.

To address this limitation, we propose Generalized Graph Information Bottleneck with Confidence Constraints (GIB-CC), a novel framework that integrates confidence into post-hoc GNN explainability. Our method dynamically quantifies explanation reliability by learning a confidence-aware representation, ensuring that explanations align with their true fidelity. Unlike ensemble-based approaches, our confidence estimation is self-contained, computationally efficient, and theoretically grounded, making it applicable to real-world scenarios where understanding both what a model predicts and how confident it is in its explanations is critical.

3 Preliminary

3.1 Notations and Problem Definition

We denote a graph as $G = (\mathcal{V}, \mathcal{E}; \mathbf{X}, \mathbf{A})$, where $\mathcal{V} = \{v_1, v_2, \dots, v_n\}$ represents a set of n nodes and $\mathcal{E} \in \mathcal{V} \times \mathcal{V}$ represents the edge set. Each graph has a feature matrix $\mathbf{X} \in \mathbb{R}^{n \times d}$ for the nodes, where in \mathbf{X} , $\mathbf{x}_i \in \mathbb{R}^{1 \times d}$ is the d -dimensional node feature of node v_i . \mathcal{E} is described by an adjacency matrix $\mathbf{A} \in \{0, 1\}^{n \times n}$. $A_{ij} = 1$ means that there is an edge between node v_i and v_j ; otherwise, $A_{ij} = 0$.

For graph classification tasks, each graph G_i has a label $Y_i \in \mathcal{C}$, with a GNN model f trained to classify G_i into its class, i.e., $f : (\mathbf{X}, \mathbf{A}) \mapsto \{1, 2, \dots, \mathcal{C}\}$.

PROBLEM 1 (POST-HOC INSTANCE-LEVEL GNN EXPLANATION). *Given a trained GNN model f , for an arbitrary input graph $G = (\mathcal{V}, \mathcal{E}; \mathbf{X}, \mathbf{A})$, the goal of post-hoc instance-level GNN explanation is to find a sub-graph G^* that can explain the prediction of f on G .*

Informative feature selection has been well studied in non-graph structured data [14], and traditional methods, such as concrete autoencoder [5], can be directly extended to explain features in GNNs. In this paper, we focus on discovering important typologies and their confidence. Formally, the obtained explanation G^* is depicted by a binary mask $\mathbf{M} \in \{0, 1\}^{n \times n}$ on the adjacency matrix \mathbf{A} , e.g., $G^* = (\mathcal{V}, \mathcal{E}, \mathbf{A} \odot \mathbf{M}; \mathbf{X})$, \odot means elements-wise multiplication. The mask highlights components of the original graph G that are essential for f to make the prediction. More importantly, we would like to obtain the confidence of explanations given \mathbf{M} and G :

PROBLEM 2 (CONFIDENCE-AWARE EXPLANATION). *Given an Explainer model E , for an arbitrary input graph $G = (\mathcal{V}, \mathcal{E}; \mathbf{X}, \mathbf{A})$ and explanation G^* , the goal of confidence scoring model f_C is giving the confidence score matrix $\mathbf{C} = \{C_{ij} | C_{ij} \in [0, 1]\} \in \mathbb{R}^{n \times n}$ that can reflect the confidence of E on edges in G^* .*

4 Methodology

The original Graph Information Bottleneck (GIB) framework provides an effective paradigm for extracting explanatory sub-graphs from a given graph G . However, existing GIB-based explainability methods lack an explicit mechanism for measuring the confidence of explanations. To address this, we introduce the Generalized Graph Information Bottleneck with Confidence Constraints (GIB-CC), which extends GIB by integrating a confidence-aware mechanism into the optimization objective.

4.1 Formalization of GIB-CC

Given a graph $G \sim P_G$ with its label $Y \sim P_Y$, and its sub-graph $G' \subseteq G$, the Graph Information Bottleneck, aiming to find the optimized explanation G^* , objective is formulated as Eq. (1):

$$G^* = \arg \min_{G'} I(G, G') - \alpha I(Y, G'), \quad (1)$$

where G^* represents the optimized explanation sub-graph, and G' denotes a candidate sub-graph. The goal is to minimize structural constraints between G and G' while retaining mutual information relevant to Y . However, this objective lacks an explicit mechanism for estimating the confidence of the explanations.

4.1.1 Confidence-aware GIB. To estimate the confidence of the explanations, we introduce a confidence matrix \mathbf{C} , which serves as a measure of the reliability of each edge in the sub-graph. We reformulate the objective with the confidence constraints as follows:

$$\begin{aligned} \arg \min_{G'} \quad & I(G, G') - \alpha I(Y, \tilde{G}), \\ & \text{where } \tilde{G} = \phi(G', \mathbf{C}) = \mathbf{C} \odot G' + (\mathbf{1} - \mathbf{C}) \odot G^r, \\ & \text{s.t. } I(\mathbf{C}, G^r; Y | G') = 0. \end{aligned} \quad (2)$$

Here, \tilde{G} is a calibrated version of the explanation sub-graph, incorporating Gaussian noise $G^r : \mathbf{A} \odot \mathbf{M}^r$ weighted by the confidence score \mathbf{C} , where each entry M_{ij}^r in \mathbf{M}^r is randomly sampled from the Gaussian distribution. The term $\mathbf{C} \odot G^r$ represents the confidence-weighted explanation over the while $(\mathbf{1} - \mathbf{C}) \odot G^r$ introduces controlled noise to calibrate uncertainty. $\mathbf{1}$ is a ones matrix with same shape as \mathbf{A} , \mathbf{M} , and \mathbf{C} . The constraints ensure that the calibrated graph retains the same level of dependency on the original graph and labels as the original explanation.

4.1.2 Mutual Information Interpretation. To further justify the role of confidence in our objective, we decompose the mutual information terms:

$$I(Y, \tilde{G}) = H(Y) - H(Y | \tilde{G}), \quad (3)$$

where the conditional entropy can be rewritten as:

$$H(Y | \tilde{G}) = H(Y | G') + I(\mathbf{C}, G^r; Y | G'). \quad (4)$$

Given G^r as an independent sampled graph noise and \mathbf{C} as an extrinsic generated score, we have $I(\mathbf{C}, G^r; Y | G') = 0$. A detailed illustration could be found in Appendix B. Therefore, we obtain:

$$H(Y | \tilde{G}) = H(Y | G'), \quad (5)$$

which ensures that our framework, with the confidence-aware formulation, maintains equivalence with the original GIB formulation. This guarantees that adding confidence constraints does not distort the explanation quality while enabling confidence estimation. Therefore, we have property (1) as follows:

Property 1. *The confidence-aware GIB objective, Eq. (2) is equivalent to vanilla GIB, Eq. (1).*

This property can be proved by considering the conditions of $I(\mathbf{C}, G^r; Y | G') = 0$, then we have:

$$H(Y | \tilde{G}) = H(Y | G^*) + I(\mathbf{C}, G^r; Y | G^*) = H(Y | G^*; \mathbf{C}, G^r).$$

Thus, the optimal solutions of GIB and our confidence-aware version are equivalent. The advantage of our objective is that by introducing the confidence matrix \mathbf{C} that weighted with the Gaussian noise G^r , we can generate the explanation sub-graph G^* with a confidence \mathbf{C} with stochasticity. Following exiting work [17, 31, 35], we can further approximate $H(Y | G^*; \mathbf{C}, G^r)$ with $\text{CE}(Y, \tilde{Y})$ in classification tasks or $\text{MSE}(Y, \tilde{Y})$ in regression tasks, where $\tilde{Y} = f \circ \phi(G^*, \mathbf{C})$ is the predicted label of \tilde{G} made by the model f . Especially when \mathbf{C} is a one's vector, our objective degenerates to the vanilla approximation. Formally, the design of the confidence evaluation model and the loss function derived from the generalized GIB-CC objective for GNN explanation are described in the following sections.

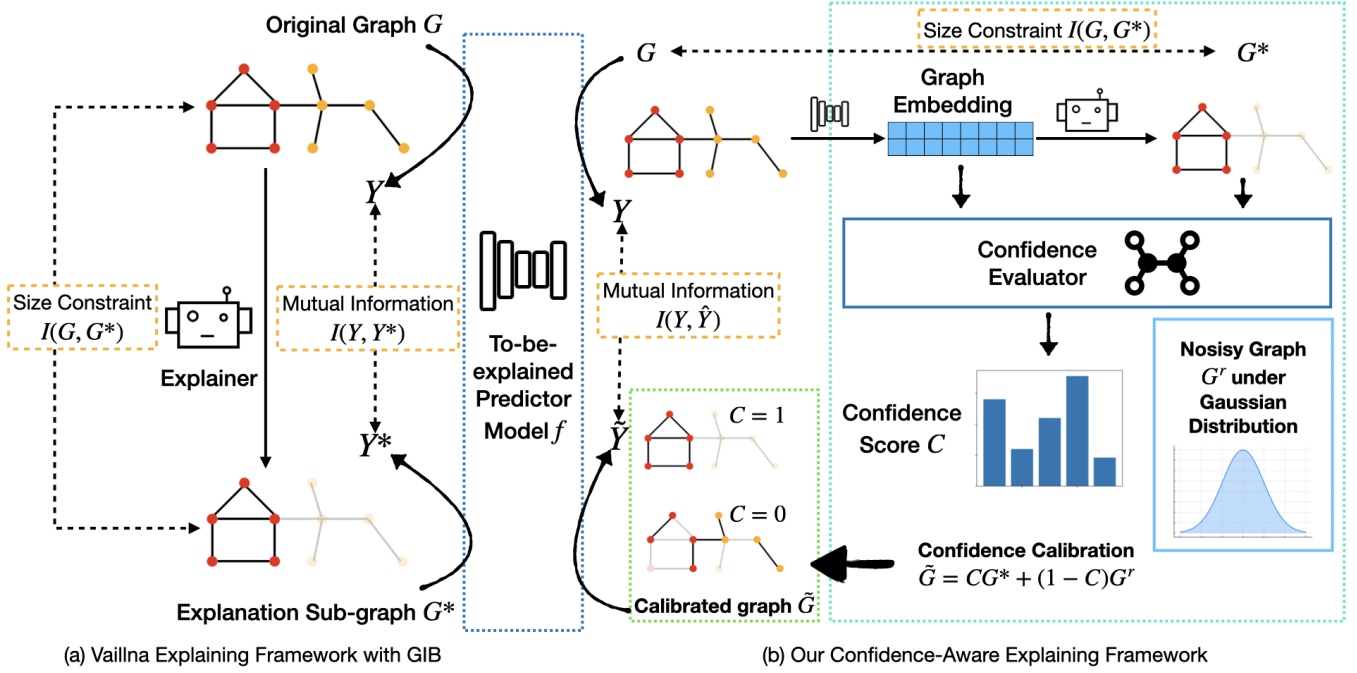


Figure 2: This figure illustrates the difference between our approach and previous approaches, based on GIB. Figure (a) on the left shows the explaining framework optimized by Graph Information Bottleneck. Figure (b) on the right shows our confidence-aware explaining framework. We first generate the explanation sub-graph G^* from the original graph G with the explainer model. Before confidence evaluation, the mask vector of edges in G^* would be concatenated with the hidden state embedding of the original graph G . After generating the confidence score C , we aggregate G^* with a random Gaussian noisy graph G^r , weight by C and $1 - C$, as \tilde{G} . Finally, we compute the confidence loss and GIB loss with C , G^* , and \tilde{G} .

4.2 Confidence Evaluation Framework

In this section, we propose our confidence-aware explaining framework based on the theoretical analysis previously.

4.2.1 Confidence Scoring Model. To quantify the reliability of explanations, we introduce a confidence scoring mechanism based on a learnable function f_C , which generates a confidence score for each edge in the explanatory sub-graph G^* . The confidence matrix is computed with an MLP and an activation layer as follows:

$$C = \text{RELU}(\text{MLP}(f_{\text{emd}}(G), \mathbf{M})), \quad (6)$$

where MLP is a multi-layer perceptron that takes the graph representation embeddings of the original graph G and its explanation mask \mathbf{M} . f_{emd} is the encoder part of the to-be-explained GNN model, where we extract the embedding before predicting. The activation function ensures that the confidence scores remain non-negative.

For each edge in G^* , the confidence score is given by $C_{ij} = \frac{1}{1+e^{-k_{ij}}}$, where k_{ij} is the raw confidence value from the MLP. This sigmoid activation ensures that confidence scores lie in the range $(0, 1)$, making them interpretable as probability estimates.

4.2.2 Loss Function. To optimize the explainer and the confidence estimator, we define a joint objective function consisting of Graph Information Bottleneck (GIB) Loss and Confidence Loss.

GIB Loss. Following prior work [17, 31], the overall loss function including the GIB loss, where the GIB loss is formulated as:

$$\mathcal{L}_{\text{GIB}} = \mathcal{L}_{\text{size}}(G, G^*) + \alpha \text{CE}(Y, f(\tilde{G})). \quad (7)$$

The first term $\mathcal{L}_{\text{size}}(G, G^*)$ ensures that the sub-graph remains compact, while the second term minimizes cross-entropy (CE) loss between the predicted label \tilde{Y} and target label Y .

Confidence Loss. We design the confidence loss based on the following principle: Given an edge prediction probability in G^* , if the classification is correct, the confidence should be high when close to the ground truth and low when far from the ground truth. Conversely, for incorrect predictions, confidence should be low when it is near the ground truth and high when it is far from it. Based on this principle, we first define a true prediction mask:

$$M_{\text{tp}}(\tilde{y}, y) = \begin{cases} 1, & \text{if } \tilde{y} \text{ is correctly classified,} \\ -1, & \text{otherwise.} \end{cases} \quad (8)$$

Using this mask, our final confidence loss is written as:

$$\mathcal{L}_C = \beta \sum M_{\text{tp},i} \frac{(C_i * (\tilde{y}_i - y)^2)}{N}, \quad (9)$$

where β is a hyperparameter controlling confidence regularization. This encourages the model to assign high confidence to correct explanations and low confidence to uncertain ones.

Final Objective. Combining both terms, our final optimization objective is:

$$\mathcal{L} = \mathcal{L}_{\text{GIB}} + \lambda \mathcal{L}_C, \quad (10)$$

where λ balances explanation quality and confidence estimation.

Training Procedure. Since the confidence loss contains both confidence score and explanation mask, to avoid of trivial solution, we train the explainer model and confidence evaluator model iteratively. When training one of them, another one is frozen. Our training algorithm is shown in Appendix C.

4.3 Time Complexity Analysis

Given the hidden state embedding e_G with shape of (d_e, d_n) of an original graph G , sub-graph explanation G^* with shape of $(\mathcal{D}_e, 1)$, and a confidence model f_C with fully connection layer which map dimension \mathcal{D}_m to 1, the complexity of concatenate of the e_g and G^* is $O(|\mathcal{D}_e|)$, where $|\mathcal{D}_e|$ denotes the number of edges or dimension of e_G of the original graph G . And the complexity of generating the confidence score is $O(|\mathcal{D}_e| * (|\mathcal{D}_n| + 1) * 1)$. For generating the confidence score, the complexity is $O(|\mathcal{D}_e| * (|\mathcal{E}_n| + 2))$. Considering the number 2 as a small constant and \mathcal{D}_n is treated as a hyper-parameter with a constant value, the overall complexity of our confidence generation is $O(|\mathcal{D}_e|)$.

5 Experimental Study

We conduct comprehensive experimental studies on benchmark datasets to empirically verify the effectiveness of the proposed ConfExplainer. Specifically, we aim to answer the following research questions: • RQ1: How does the proposed method perform compared to the baseline methods? • RQ2: Can the proposed framework generate better confidence scores? • RQ3: How do the confidence-aware explanations look like? Is it visually correct?

In addition to research questions, we conduct the experiments, including training time cost comparison, ablation study, and hyper-parameter tuning, which are put in the appendix.


5.1 Experiment Settings

5.1.1 Datasets. We evaluate our proposed ConfExplainer on a synthetic graph dataset and multiple real-world graph datasets that come with ground-truth explanations. The synthetic dataset, BA-2motifs, is used for graph classification tasks, providing a controlled environment to evaluate explanation methods. The real-world datasets, such as MUTAG, Benzene, Fluoride-Carbonyl, and Alkane-Carbonyl, consist of molecular graphs and are designed to determine whether a molecule graph contains a specific pattern that affects molecular properties [2]. These datasets are widely used in GNN explainability and provide a reliable benchmark for assessing the quality of generated explanations.

• **BA-2motifs** A synthetic graph dataset based on the Barabási-Albert (BA) model [3], designed for node classification tasks. Each graph contains one of two possible motifs: a 5-node cycle or a 6-node ‘house’ structure, which is randomly attached to a node in a BA base graph. The classification task is to determine whether a given node belongs to one of these motif structures.

• **MUTAG** [12] A real-world chemistry dataset consisting of molecular graphs for graph-level classification, where nodes represent

atoms and edges represent chemical bonds. The objective is to classify molecules on the basis of their mutagenic properties. The presence of specific chemical substructures serves as ground-truth explanations for model predictions.

• **Benzene** [21] A molecular dataset where the task is to classify molecules based on the presence of benzene rings (). The ground-truth explanations highlight the benzene substructures responsible for the graph-level classification.

• **Fluoride-Carbonyl** [21] A molecular dataset where the objective is to classify molecules based on the presence of fluoride and carbonyl functional groups. The ground-truth explanations focus on identifying these functional groups within the molecular graphs.

• **Alkane-Carbonyl** [21] A molecular dataset where the graph-level classification task is based on the presence of an unbranched alkane and a carbonyl functional groups (C=O). The explanations aim to highlight the structure responsible for the classification.

For detailed information on dataset loading and usage, refer to the G-XAI Bench repository [20] and associated documentation.

5.1.2 Baselines. To evaluate the effectiveness of ConfExplainer, we compare it against four baseline methods. GNNExplainer (GNNE) and PGExplainer (PGE) are widely used post-hoc explainability methods for GNNs. Additionally, we include two ensemble-based baselines, which are popular techniques for uncertainty estimation. These methods allow us to evaluate both the quality of our explanations and the reliability of our confidence scores.

• **GNNE** [31]: A widely used post-hoc explainability method that identifies key sub-graphs responsible for a GNN’s predictions. It learns an edge mask by optimizing for fidelity while preserving the model’s original predictions.

• **PGE** [17]: A parameterized graph explainer that learns a probabilistic mask distribution over graph edges. Unlike GNNExplainer, PGExplainer incorporates a global view of the dataset by training an explainer network that generalizes across instances.

• **Deep Ensemble** [13]: A well-established uncertainty quantification method that trains multiple independent GNNs with different initializations. The ensemble’s variance provides an estimate of prediction uncertainty, but it does not inherently produce explanations for model decisions. We use it as a baseline to compare our confidence-aware explanation quality.

• **Bootstrap Ensemble** [1]: In this approach, multiple models are trained on different bootstrap samples of the dataset. Bootstrapping is particularly useful when the base model lacks intrinsic randomness, as it helps introduce diversity among ensemble members. In our setup, we apply a k-fold ensemble strategy to evaluate the baseline explainers. Specifically, we split the dataset into k fold, train the baseline explainer with $k - 1$ fold k times, and evaluate it on the rest 1 fold. Then we calculate metrics with the mean value of each edge weight on the test graphs with the k results.

5.1.3 Configurations. The experiment configurations are set following prior research [37]. A three-layer GCN model was trained on 80% of each dataset’s instances as the target model. We apply the same hyper-parameters for all methods: The learning rate was initialized to 0.005, with 30 training epochs. The regularization coefficients are 0.0003 and 0.3. Specifically, the weight of confidence loss for our approach is 100. Explanations are tested in all instances.

Table 1: Comparison of AUC-ROC (\uparrow) performance on five datasets. The best results are highlighted in bold. The second-best results are underlined. ConfExplainer achieves the best performance in BA-2motifs, MUTAG, Fluoride-Carbonyl and Alkane-Carbonyl, while holds a comparable performance in Benzene.

Dataset	GNNE	PGE	Deep Ensemble	Bootstrap Ensemble	ConfExplainer
BA-2motifs	54.58% \pm 1.21%	88.15% \pm 0.69%	80.47% \pm 1.20%	81.56% \pm 0.96%	97.19% \pm 0.04%
MUTAG	59.77% \pm 0.67%	65.31% \pm 8.78%	<u>68.78% \pm 1.16%</u>	68.63% \pm 1.53%	90.14% \pm 0.97%
Benzene	50.40% \pm 0.30%	77.57% \pm 1.43%	78.60% \pm 0.24%	<u>78.11% \pm 0.24%</u>	77.80% \pm 1.32%
Fluoride-Carbonyl	54.72% \pm 0.67%	54.78% \pm 4.42%	52.59% \pm 1.11%	<u>55.70% \pm 1.61%</u>	59.27% \pm 1.48%
Alkane-Carbonyl	54.03% \pm 2.13%	73.05% \pm 2.00%	74.44% \pm 0.18%	<u>75.17% \pm 0.33%</u>	81.52% \pm 0.22%

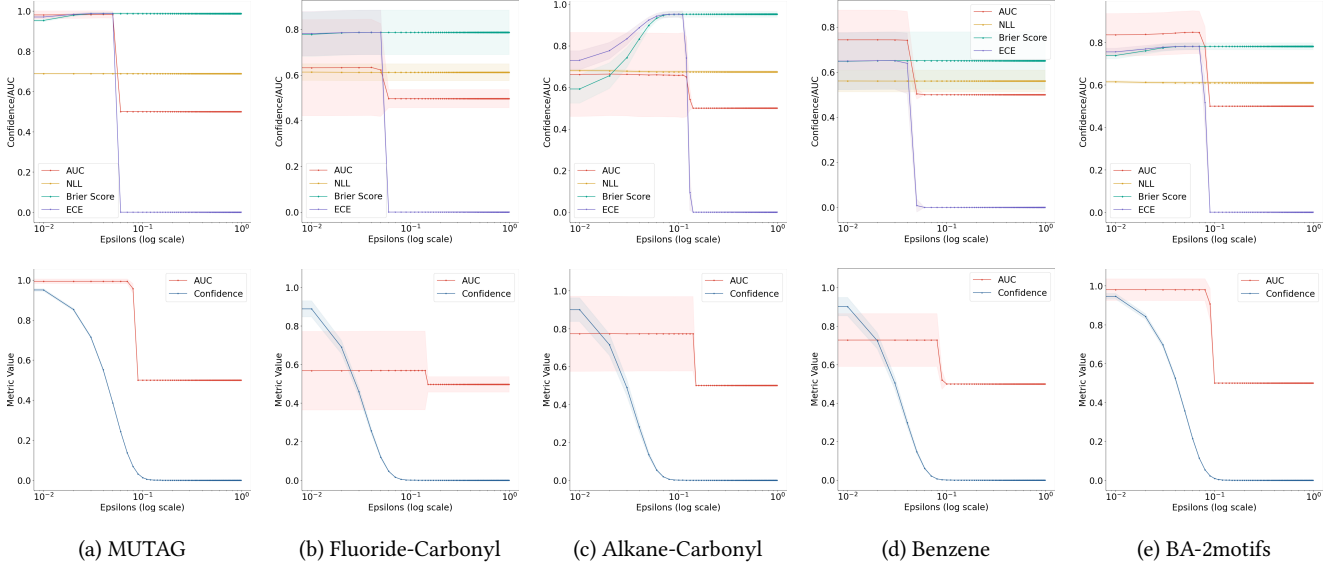


Figure 3: Visualization of AUC, NLL, BR, ECE, and confidence score of baseline PGEexplainer and ConfExplainer on five datasets. Each metric is computed at the graph level and plotted with mean and std in the sub-figures. The x-axis in the sub-figures denotes the noise level $\epsilon \in [0, 1]$ in the log scale, and the y-axis denotes the value of AUC, NLL, BR, ECE, and confidence score.

The experiments are conducted on a Linux server with Ubuntu 16.04, 32 cores Intel(R) Xeon(R) CPU E5-2620 v4 @ 2.10GHz, and NVIDIA TITAN Xp 12 GB GPU.

5.1.4 Evaluation Metrics. To assess the performance of our proposed ConfExplainer and baselines, we evaluate the quality of explanations with AUC-ROC score and the reliability of confidence scores using the following metrics: Negative Log-Likelihood (NLL), Briers Score (BR), and Expected Calibration Error (ECE). Detailed description is attached in the Appendix D.

5.2 Quantitative Evaluation on Explanation Faithfulness (RQ1)

To address RQ1, we compare our proposed approach with multiple baseline methods, evaluating explanation faithfulness using the AUC-ROC metric. The AUC-ROC score is computed by evaluating the weighted vector of the graph explanation against the ground truth. Each experiment is conducted 10 times with different random seeds, and we report the mean performance and standard deviations in Table 1. We have the following observations:

- In BA-2motifs, MUTAG, Fluoride-Carbonyl, and Alkane-Carbonyl, our method achieves the best AUC-ROC scores compared to baseline explainability methods, including GNNEexplainer, PGExplainer, and ensemble approaches. Our model significantly outperforms these baselines in explanation quality, demonstrating its ability to produce more faithful and interpretable graph explanations.
- Specifically, our approach improves AUC scores by 21.00% and 24.52% on average, with particularly strong performance gains on datasets such as BA-2motifs and MUTAG. This highlights that our confidence-aware framework generates more accurate and reliable explanations, aligning better with the underlying ground truth.
- In Benzene dataset, the Deep Ensemble approach retrieved the best AUC, but our method still has a comparable performance, since our method emphasizes confidence scoring while maintaining comparable accuracy.

5.3 Confidence Scoring and Calibration

In this section, we answer the RQ2 with two parts of experiments: (1) we compared our method with baseline methods on the confidence metrics including NLL, BR, and ECE. This a static experiment,

Table 2: Comparison of NLL (\downarrow), BR (\downarrow), and ECE (\downarrow) on five datasets. Lower values indicate better performance.

Dataset	Metric	GNNE	PGE	Deep Ensemble	Bootstrap Ensemble	ConfExplainer
BA-2motifs	NLL	0.7197 ± 0.0005	0.6318 ± 0.0081	0.6171 ± 0.0007	0.6193 ± 0.0012	0.6117 ± 0.0008
	BR	0.2449 ± 0.0011	0.5705 ± 0.0397	0.7205 ± 0.0046	0.6996 ± 0.0085	0.7340 ± 0.0177
	ECE	0.2714 ± 0.0009	0.6553 ± 0.0290	0.7480 ± 0.0023	0.7337 ± 0.0062	0.7858 ± 0.0100
MUTAG	NLL	0.6965 ± 0.0000	0.6832 ± 0.0004	0.6831 ± 0.0000	0.6832 ± 0.0000	0.6829 ± 0.0001
	BR	0.2413 ± 0.0001	0.9275 ± 0.0276	0.9335 ± 0.0022	0.9282 ± 0.0017	0.9375 ± 0.0125
	ECE	0.4630 ± 0.0001	0.9490 ± 0.0149	0.9523 ± 0.0012	0.9496 ± 0.0009	0.9546 ± 0.0065
Benzene	NLL	0.7143 ± 0.0001	0.6203 ± 0.0004	0.6202 ± 0.0001	0.6203 ± 0.0001	0.6201 ± 0.0004
	BR	0.2620 ± 0.0003	0.7931 ± 0.0063	0.7887 ± 0.0012	0.7910 ± 0.0010	0.7910 ± 0.0061
	ECE	0.3158 ± 0.0003	0.7985 ± 0.0036	0.7960 ± 0.0007	0.7973 ± 0.0006	0.7973 ± 0.0035
Fluoride-Carbonyl	NLL	0.6979 ± 0.0001	0.6789 ± 0.0001	0.6789 ± 0.0000	0.6789 ± 0.0001	0.7166 ± 0.0001
	BR	0.2393 ± 0.0005	0.9471 ± 0.0075	0.9460 ± 0.0011	0.9442 ± 0.0010	0.0378 ± 0.0002
	ECE	0.4446 ± 0.0005	0.9541 ± 0.0039	0.9535 ± 0.0006	0.9526 ± 0.0006	0.0318 ± 0.0025
Alkane-Carbonyl	NLL	0.6959 ± 0.0001	0.6884 ± 0.0007	0.6887 ± 0.0001	0.6888 ± 0.0001	0.7052 ± 0.0002
	BR	0.2422 ± 0.0015	0.5051 ± 0.0822	0.4623 ± 0.0088	0.4662 ± 0.0100	0.0213 ± 0.0002
	ECE	0.4643 ± 0.0015	0.6762 ± 0.0635	0.4652 ± 0.0080	0.6502 ± 0.0090	0.0094 ± 0.0018

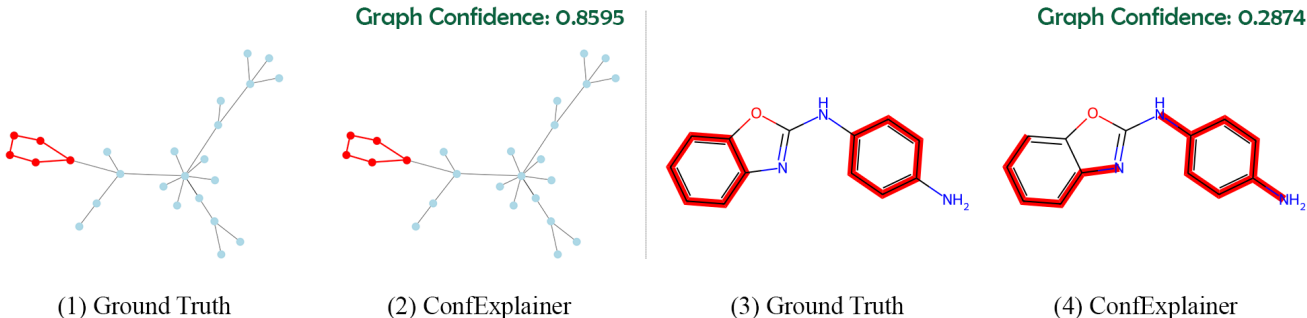


Figure 4: Visualization of two graph case studies using ConfExplainer. On the left (1 and 2), with samples from the BA-2motifs dataset, our model successfully identifies the "house" structure, highlighted in red, with a relatively high confidence score (0.8595). On the right (3 and 4), with samples from the Benzene dataset, our model fails to accurately detect the significant substructure in the chemical graph with a lower confidence score (0.2874).

where we generate the explanation for original graph instances and compute the metrics with ground truth labels. The results are shown in Table 2, more analysis is conducted below; (2) to further demonstrate the effectiveness of our proposed method, we introduce the OOD scenario by injecting the noise into the original graphs. With the increasing noise level, we visualize the explanation accuracy and model confidence. Specifically, we add noise in the edge feature level by disturbing the node feature with a consistent value ϵ . The higher ϵ is, the more OOD the original graph is, which would make it harder for trained models to recognize the explanation sub-graph, and the explainer confidence should decrease as well. The results are shown in Figure 3, wherein the first row, we plot the AUC score and confidence evaluation metrics, including NLL, BR, and ECE of plain PGExplainer; in the second row, we visualize our proposed approach with AUC and confidence score generated by the confidence scoring model.

We have the following observations:

- The confidence score could better evaluate the confidence of the explainer model, as it shows a decreasing tendency while adding

more noise and the performance of the explainer is dropping, as shown in Figure 3, while NLL and BR couldn't reflect. Moreover, the confidence score decreases smoothly when more noise is injected, while ECE only drop-down at the critical point; The reason for ConfExplainer not performing best in Table 2 is these metrics rely more on the concept of uncertainty, which is different from confidence, and it's not specifically optimized by our approach.

- Unlike previous confidence evaluation metrics, which require access to ground truth explanations for score computation, our proposed confidence scoring model operates independently of ground truth. This key advantage enables our approach to effectively assess the confidence of explanations in out-of-distribution (OOD) scenarios or on newly encountered datasets, where ground truth explanations may be unavailable. The reason our method does not achieve the highest performance in Table 2 is that existing uncertainty-based metrics are primarily designed to capture prediction uncertainty, which is conceptually distinct from explanation confidence. Since our approach is not explicitly optimized

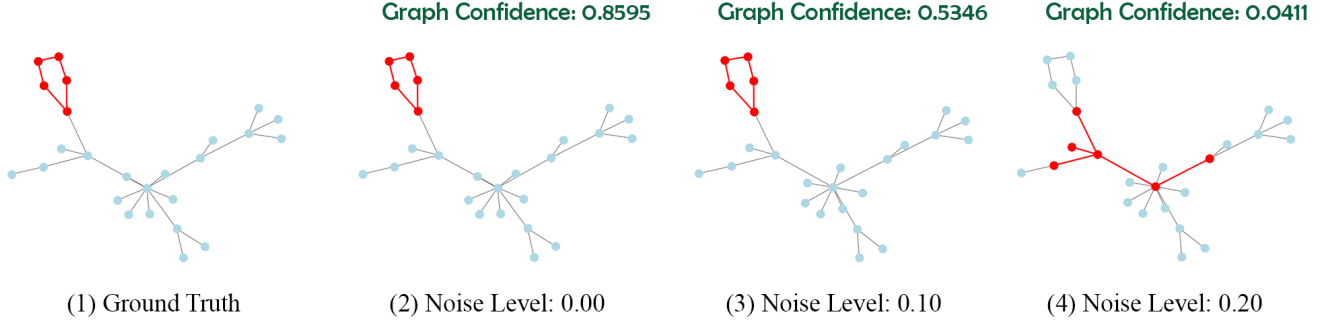


Figure 5: Visualization of the impact of different noise levels on the confidence scores and explanations provided by ConfExplainer. This figure shows that as the noise level increases from 0.00 to 0.20, the model’s confidence score drops significantly from 0.8595 to 0.5346, and finally to 0.0411. At higher noise levels, the model faces difficulty in accurately identifying the ground truth structure, as illustrated in (4).

for uncertainty estimation, these metrics do not fully reflect the improvements brought by our confidence-aware framework.

- By training the explainer with the confidence model, the explainer is more robust on the slight noise disturbing. The rash point is larger for ConfExplainer than the baseline PGExplainer, and the converged AUC value is 0.5, a random result, compared to the 0.0 in the first row, where PGExplainer gives the fully opposite results. In conclusion, our confidence model effectively evaluates the explainer’s confidence and improves its robustness.

5.4 Case Study: Could the confidence score reveal the explainer’s performance? (RQ3)

In this section, we showcase the confidence score and explanation from the explainer (ConfExplainer) in two perspectives: The first part includes the static result, where we visualize the result from different graphs; the second part includes the noise injection, where we visualize the compression of one graph with different levels of the noise. Both part is drawn with the original graph, highlighted top-k explanation edges, and paired confidence score.

5.4.1 Static Study. As shown in Figure 4, the left and right sides visualize examples from two different datasets. Figure 4(1) and Figure 4(2) correspond to the BA-2motifs dataset, where the explanation is both accurate and associated with a high confidence score. In contrast, Figure 4(3) and Figure 4(4) correspond to the Benzene dataset, where the explanation is discrete and accompanied by a low confidence score. In Figure 4(1) and Figure 4(3), the red-highlighted edges represent the ground-truth explanations. Figure 4(2) and Figure 4(4) illustrate the results produced by ConfExplainer, including the predicted explanations (highlighted) and the corresponding graph confidence scores. This observation aligns with the results presented in the previous table, demonstrating that the confidence module effectively evaluates the reliability of model explanations. Additional examples from more datasets can be found in the appendix Figure 7.

5.4.2 Noise Injection. To visualize the effect of the noise injection, we conduct an experiment on injecting the noise into the graph embedding before feeding it into the explainer, and observing the

change of the explanation fidelity and confidence. We randomly sample a graph from the dataset BA-2motifs for the case study. As observed in Figure 5. As more noise is injected into the graph embedding, the explainer’s confidence decreases steadily, while the explanation accuracy initially remains stable but eventually collapses at a higher noise level, when the noise level increase from 0.1 to 0.2, aligning with the observation in Figure 3. It’s aligned with the hypothesis that with the noise injection, the explainers’ performance and confidence would decrease in parallel, indicating the effectiveness of our confidence evaluation module.

6 Conclusion

In this work, we addressed a critical gap in Graph Neural Network (GNN) explainability by introducing a confidence-aware explanation framework, Generalized Graph Information Bottleneck with Confidence Constraints (GIB-CC). While existing GNN explainers provide insights into model decisions, they often fail to quantify the trustworthiness of their explanations. Our approach explicitly integrates confidence estimation into the explanation process, ensuring that users can assess not only what a model explains but also how reliable that explanation is. Through extensive theoretical analysis and empirical validation, we demonstrated that our framework significantly improves both explanation faithfulness and confidence calibration. Our confidence evaluation module enhances explanation reliability, enabling better differentiation between high-fidelity and low-fidelity explanations, particularly in out-of-distribution (OOD) scenarios. Moreover, our confidence-aware training strategy improves the robustness of GNN explainers, mitigating performance degradation under distribution shifts.

Looking forward, our work paves the way for further trustworthy AI research in graph-based learning. Future directions include extending our confidence-aware framework to dynamic and evolving graphs, exploring more efficient confidence estimation techniques, and integrating confidence-aware explanations into real-world applications such as drug discovery, fraud detection, and decision support systems. By bridging the gap between explainability and reliability, we hope to contribute to the broader adoption of trustworthy and interpretable GNNs in high-stakes domains.

ACKNOWLEDGMENTS

The work was partially supported by NSF awards #2421839, NAIRR #240120, and NSF No. IIS-2331908. This work used AWS through the CloudBank project, which is supported by National Science Foundation grant #1925001. The views and conclusions contained in this paper are those of the authors and should not be interpreted as representing any funding agencies. We thank OpenAI for providing us with API credits under the Researcher Access program and Amazon Research Awards.

References

- [1] Moloud Abdar, Farhad Pourpanah, Sadiq Hussain, Dana Rezazadegan, Li Liu, Mohammad Ghavamzadeh, Paul Fieguth, Xiaochun Cao, Abbas Khosravi, U Rajendra Acharya, et al. 2021. A review of uncertainty quantification in deep learning: Techniques, applications and challenges. *Information fusion* 76 (2021), 243–297.
- [2] Chirag Agarwal, Owen Queen, Himabindu Lakkaraju, and Marinka Zitnik. 2023. Evaluating explainability for graph neural networks. *Scientific Data* 10, 1 (2023), 144.
- [3] Réka Albert and Albert-László Barabási. 2002. Statistical mechanics of complex networks. *Reviews of modern physics* 74, 1 (2002), 47.
- [4] Federico Baldassarre and Hossein Azizpour. 2019. Explainability Techniques for Graph Convolutional Networks.
- [5] Muhammed Fatih Balın, Abubakar Abid, and James Zou. 2019. Concrete autoencoders: Differentiable feature selection and reconstruction. In *International conference on machine learning*. PMLR, 444–453.
- [6] Glenn W Brier. 1950. Verification of forecasts expressed in terms of probability. *Monthly weather review* 78, 1 (1950), 1–3.
- [7] Zhuomin Chen, Jiaxing Zhang, Jingchao Ni, Xiaoting Li, Yuchen Bian, Md Mezbahul Islam, Ananda Mondal, Hua Wei, and Dongsheng Luo. 2024. Generating In-Distribution Proxy Graphs for Explaining Graph Neural Networks. In *Forty-first International Conference on Machine Learning*. <https://openreview.net/forum?id=ohG9bVMs5j>
- [8] Enyan Dai and Suhang Wang. 2021. Towards Self-Explainable Graph Neural Network.
- [9] Enyan Dai, Tianxiang Zhao, Huaisheng Zhu, Junjie Xu, Zhimeng Guo, Hui Liu, Jiliang Tang, and Suhang Wang. 2024. A comprehensive survey on trustworthy graph neural networks: Privacy, robustness, fairness, and explainability. *Machine Intelligence Research* 21, 6 (2024), 1011–1061.
- [10] Vincenzo Marco De Luca, Antonio Longa, Pietro Lio, and Andrea Passerini. [n. d.]. xAI-Drop: Don't use what you cannot explain. In *The Third Learning on Graphs Conference*.
- [11] Wenqi Fan, Yao Ma, Qing Li, Yuan He, Eric Zhao, Jiliang Tang, and Dawei Yin. 2019. Graph Neural Networks for Social Recommendation.
- [12] Jeroen Kazius, Ross McGuire, and Roberta Bursi. 2005. Derivation and validation of toxicophores for mutagenicity prediction. *Journal of medicinal chemistry* 48, 1 (2005), 312–320.
- [13] Balaji Lakshminarayanan, Alexander Pritzel, and Charles Blundell. 2017. Simple and scalable predictive uncertainty estimation using deep ensembles. *Advances in neural information processing systems* 30 (2017).
- [14] Jundong Li, Kewei Cheng, Suhang Wang, Fred Morstatter, Robert P. Trevino, Jiliang Tang, and Huan Liu. 2017. Feature Selection: A Data Perspective. *ACM Comput. Surv.* 50, 6, Article 94 (dec 2017), 45 pages. <https://doi.org/10.1145/3136625>
- [15] Mengzhang Li and Zhanxing Zhu. 2021. Spatial-Temporal Fusion Graph Neural Networks for Traffic Flow Forecasting. *Proceedings of the AAAI Conference on Artificial Intelligence* 35, 5 (May 2021), 4189–4196.
- [16] Yang Li, Buyue Qian, Xianli Zhang, and Hui Liu. 2020. Graph neural network-based diagnosis prediction. *Big data* 8, 5 (2020), 379–390.
- [17] Dongsheng Luo, Wei Cheng, Dongkuan Xu, Wenchao Yu, Bo Zong, Haifeng Chen, and Xiang Zhang. 2020. Parameterized explainer for graph neural network. *Advances in neural information processing systems* 33 (2020), 19620–19631.
- [18] Siqi Miao, Mia Liu, and Pan Li. 2022. Interpretable and generalizable graph learning via stochastic attention mechanism. In *International Conference on Machine Learning*. PMLR, 15524–15543.
- [19] Shengjie Min, Zhan Gao, Jing Peng, Liang Wang, Ke Qin, and Bo Fang. 2021. STGSN — A Spatial-Temporal Graph Neural Network framework for time-evolving social networks. *Knowledge-Based Systems* 214 (2021), 106746.
- [20] Owen Queen. 2022. GraphXAI. <https://doi.org/10.7910/DVN/KULOS8>
- [21] Benjamin Sanchez-Lengeling, Jennifer Wei, Brian Lee, Emily Reif, Peter Wang, Wesley Qian, Kevin McCloskey, Lucy Colwell, and Alexander Wiltchko. 2020. Evaluating attribution for graph neural networks. *Advances in neural information processing systems* 33 (2020), 5898–5910.
- [22] Caihua Shan, Yifei Shen, Yao Zhang, Xiang Li, and Dongsheng Li. 2021. Reinforcement Learning Enhanced Explainer for Graph Neural Networks. In *Advances in Neural Information Processing Systems*, A. Beygelzimer, Y. Dauphin, P. Liang, and J. Wortman Vaughan (Eds.). <https://openreview.net/forum?id=nUtlCcV24hL>
- [23] Indro Spinelli, Simone Scardapane, and Aurelio Uncini. 2022. A meta-learning approach for training explainable graph neural networks. *IEEE Transactions on Neural Networks and Learning Systems* (2022).
- [24] Ronast Subedi, Lu Wei, Wenhan Gao, Shayok Chakraborty, and Yi Liu. 2024. Empowering Active Learning for 3D Molecular Graphs with Geometric Graph Isomorphism. In *Advances in Neural Information Processing Systems*, A. Globerson, L. Mackey, D. Belgrave, A. Fan, U. Paquet, J. Tomczak, and C. Zhang (Eds.), Vol. 37. Curran Associates, Inc., 55507–55537. https://proceedings.neurips.cc/paper_files/paper/2024/file/6462073c6bdf864ebfbb11e80619f3e-Paper-Conference.pdf
- [25] Fangxin Wang, Yuqing Liu, Kay Liu, Yibo Wang, Sourav Medya, and Philip S Yu. 2024. Uncertainty in Graph Neural Networks: A Survey. *arXiv preprint arXiv:2403.07185* (2024).
- [26] Xiaoyang Wang, Yao Ma, Yiqi Wang, Wei Jin, Xin Wang, Jiliang Tang, Caiyan Jia, and Jian Yu. 2020. Traffic Flow Prediction via Spatial Temporal Graph Neural Network. In *Proceedings of The Web Conference 2020 (Taipei, Taiwan) (WWW '20)*. Association for Computing Machinery, New York, NY, USA, 1082–1092.
- [27] Xiang Wang, Yingxin Wu, An Zhang, Xiangnan He, and Tat-seng Chua. 2021. Causal screening to interpret graph neural networks. (2021).
- [28] Tailin Wu, Hongyu Ren, Pan Li, and Jure Leskovec. 2020. Graph information bottleneck. *Advances in Neural Information Processing Systems* 33 (2020), 20437–20448.
- [29] Zonghan Wu, Shirui Pan, Guodong Long, Jing Jiang, and Chengqi Zhang. 2019. Graph Wavenet for Deep Spatial-Temporal Graph Modeling. In *Proceedings of the 28th International Joint Conference on Artificial Intelligence (Macao, China) (IJCAI'19)*. AAAI Press, 1907–1913.
- [30] Liu Xufeng, Luo Dongsheng, Gao Wenhan, and Liu Yi. 2024. 3DGraphX: Explaining 3D Molecular Graph Models via Incorporating Chemical Priors. In *Proceedings of the 31th ACM SIGKDD Conference on Knowledge Discovery and Data Mining (IJCAI'19)*. AAAI Press, 1907–1913.
- [31] Zhitao Ying, Dylan Bourgeois, Jiaxuan You, Marinka Zitnik, and Jure Leskovec. 2019. Gnnexplainer: Generating explanations for graph neural networks. *Advances in neural information processing systems* 32 (2019). <https://doi.org/10.48550/ARXIV.1903.03894>
- [32] Bing Yu, Haoteng Yin, and Zhanxing Zhu. 2018. Spatio-Temporal Graph Convolutional Networks: A Deep Learning Framework for Traffic Forecasting. In *Proceedings of the Twenty-Seventh International Joint Conference on Artificial Intelligence, IJCAI-18*. International Joint Conferences on Artificial Intelligence Organization, 3634–3640.
- [33] Junchi Yu, Tingyang Xu, Yu Rong, Yatao Bian, Junzhou Huang, and Ran He. 2020. Graph information bottleneck for subgraph recognition. *arXiv preprint arXiv:2010.05563* (2020).
- [34] Hao Yuan, Haiyang Yu, Jie Wang, Kang Li, and Shuiwang Ji. 2021. On explainability of graph neural networks via subgraph explorations. In *International Conference on Machine Learning*. PMLR, 12241–12252.
- [35] Jiaxing Zhang, Zhuomin Chen, hao mei, Longchao Da, Dongsheng Luo, and Hua Wei. 2024. RegExplainer: Generating Explanations for Graph Neural Networks in Regression Tasks. In *Advances in Neural Information Processing Systems*, Vol. 37. Curran Associates, Inc., 79282–79306.
- [36] Jiaxing Zhang, Jiayi Liu, Dongsheng Luo, Jennifer Neville, and Hua Wei. 2024. LLMExplainer: Large Language Model based Bayesian Inference for Graph Explanation Generation.
- [37] Jiaxing Zhang, Dongsheng Luo, and Hua Wei. 2023. MixupExplainer: Generalizing Explanations for Graph Neural Networks with Data Augmentation. In *Proceedings of 29th ACM SIGKDD Conference on Knowledge Discovery and Data Mining (SIGKDD)*.
- [38] Xin Zhang, Zhen Xu, Yue Liu, Mengfang Sun, Tong Zhou, and Wenying Sun. 2024. Robust Graph Neural Networks for Stability Analysis in Dynamic Networks. In *2024 3rd International Conference on Cloud Computing, Big Data Application and Software Engineering (CBASE)*. IEEE, 806–811.
- [39] Jie Zhou, Ganqu Cui, Shengding Hu, Zhengyan Zhang, Cheng Yang, Zhiyuan Liu, Lifeng Wang, Changcheng Li, and Maosong Sun. 2020. Graph neural networks: A review of methods and applications. *AI open* 1 (2020), 57–81.

A Notation Table

Symbol	Description
$G = (\mathcal{V}, \mathcal{E}; X, A)$	Original Graph
\mathcal{E}	Edge set
X	Feature matrix
A	Adjacency matrix
M	Binary mask
G'	Candidate sub-graph
\tilde{G}	Calibrated sub-graph
G^r	Gaussian noise
Y	Target label
\tilde{Y}	Predicted label
A	Adjacency matrix of the graph
$I(\cdot)$	The mutual information
G^*	Explanation sub-graph
C	Confidence vector
c_i	Confidence score on each edge
x_i	Raw confidence score from MLP
λ	Balance between explanation and confidence
\odot	Element-wise product
$H(\cdot)$	Entropy
$CE(\cdot)$	Cross-Entropy loss
\mathcal{L}	Loss function
$f(\cdot)$	Confidence model
e	Hidden state embedding
\mathcal{D}	Dimension
\mathcal{O}	Time complexity
\mathcal{B}_k	Bin
$[l_k, u_k]$	Prediction confidence interval
C_{AN}	Correlation between AUC and NLL
C_{AB}	Correlation between AUC and BR
C_{AE}	Correlation between AUC and ECE

Table 3: Notation Table

B Justification of $I(C, G^r; Y | G') = 0$

The core assumption $I(C, G^r; Y | G') = 0$ underpins the theoretical equivalence between GIB and GIB-CC. To justify this condition, we begin with the fact that G^r is sampled as independent random Gaussian noise, and hence shares no mutual information with Y or G' . This leads to the simplification:

$$I(C, G^r; Y | G') = I(C; Y | G')$$

We further expand this mutual information term:

$$I(C; Y | G') = H(C | G') - H(C | Y, G')$$

The confidence matrix C is defined as:

$$C = \text{MLP}(f_{\text{emb}}(G), G'),$$

where $f_{\text{emb}}(G)$ is the embedding of the input graph. This implies that any dependence between C and Y must pass through G . Under the vanilla GIB assumption, we have

$$I(Y; G | G') = 0 \quad \text{i.e., } G'$$

capturing all label-relevant information from G . Since C is a deterministic function of G and G' , it follows that once G' is given, C cannot capture additional information about Y , yielding: $I(C; Y | G') = 0$. Thus, our assumption $I(C, G^r; Y | G') = 0$ is a natural extension of the GIB formulation under its own information bottleneck condition.

Moreover, the condition $I(C, G^r; Y | G') = 0$ may not strictly hold in all cases – for example, under severe OOD shifts where G' fails to retain label-relevant information. However, this limitation originates from the standard GIB formulation itself, rather than our proposed extension. Weaker or relaxed variants of this assumption would be explored in future work to enhance robustness in more general settings.

C Training Procedure

Since the confidence loss contains both confidence score and explanation mask, to avoid of trivial solution, we train the explainer model and confidence evaluator model iteratively. When training one of them, another one is frozen. Our training algorithm is shown in Algorithm 1.

Algorithm 1 Training Algorithm

Input: Target to-be-explained graph set \mathcal{G} , to-be-explained GNN model f , explainer model E , confidence model c , training epochs e .

Output: Trained explainer E and confidence evaluator c .

```

1: Initialize explainer model  $E$  and confidence evaluator model  $c$ .
2: for  $epoch \in 2 * e$  do
3:   for  $G \in \mathcal{G}$  do
4:      $G^r \leftarrow$  Randomly sampled graph Gaussian noise from  $\mathcal{N}(0, 1)$ 
5:      $H \leftarrow f(G)$ 
6:      $G^* \leftarrow E(H)$ 
7:      $C \leftarrow c(H, G^*)$ 
8:      $\tilde{G} \leftarrow CG^* + (1 - C)G^r$ 
9:     Compute  $\mathcal{L}_{\text{GIB}}(G, G^*, \tilde{G})$ 
10:    Compute  $\mathcal{L}_C(C, G^*)$ 
11:   end for
12:   if  $epoch \% 2 == 0$  then
13:     Update  $E$  with back propagation.
14:   else
15:     Update  $c$  with back propagation.
16:   end if
17: end for
18: return Explainer  $E$ , confidence evaluator  $c$ 

```

D Evaluation Metrics

To assess the performance of ConfExplainer and baselines, we evaluate the quality of explanations with AUC-ROC score and the reliability of confidence scores using the following metrics: Negative Log-Likelihood (NLL), Briers Score (BS), and Expected Calibration Error (ECE):

- Area Under the Receiver Operating Characteristic Curve (AUROC): Measures the quality of explanations generated

by the explainer. A higher AUROC indicates that the method effectively identifies meaningful substructures contributing to predictions.

- **Negative Log-Likelihood (NLL):** Evaluates the confidence scores by measuring how well the predicted probabilities align with the ground truth. The NLL is defined as: $NLL = -\frac{1}{N} \sum_{i=1}^N \log p_i$, where N is the total number of samples and p_i is the predicted probability for each sample. Lower NLL values indicate better confidence estimation performance.
- **Briers Score (BR) [6]:** BS is the mean squared error between the predicted probability and ground-truth label $\frac{1}{K} \sum_y (p_\theta(y|x_n) - \mathbf{1}_{y=y_n})^2$, where $\mathbf{1}$ is the indicator function. It serves as another proper scoring rule for classification tasks. Lower values indicating better performance.
- **Expected Calibration Error (ECE):** Measures the discrepancy between predicted confidence and actual accuracy across different confidence bins. $ECE = \sum_{k=1}^K \frac{|B_k|}{n} \hat{\epsilon}_k$,

$$\hat{\epsilon}_k = \frac{1}{|B_k|} \left| \sum_{i \in B_k} [\mathbb{1}(\hat{y}_i == y_i) - p_i] \right|$$
, where $p \in [l_k, u_k]$, B_k denotes the bin with prediction confidences bounded between l_k and u_k . A lower ECE suggests better confidence scores.
- **Pearson Correlation:** Measures the correlation between confidence scores and explanation quality. A higher correlation indicates that the explainer’s confidence aligns well with the actual quality of explanations, ensuring reliability in uncertainty estimation.

E Time Complexity

In addition to the inference cost, this section contains a complete time complexity analysis and empirical evaluation of the training overhead of the full framework.

Formally, the training complexity consists of: 1. The explainer and confidence evaluator, both implemented as MLPs operating on graph embeddings and masks, each with complexity $\mathcal{O}(|E|d)$, where $|E|$ is the number of edges and d is the embedding dimension. 2. The calibrated graph construction involves a weighted sum: $\tilde{G} = C \odot G' + (1 - C) \odot G''$, with complexity $\mathcal{O}(|E|)$. 3. Total training cost per iteration is thus linear in the graph size: $\mathcal{O}(|E|d)$, consistent with prior works like PGExplainer.

Table 4 compares wall-clock training time with PGExplainer and PGExplainer with Bootstrap-Ensemble/Deep-Ensemble in all datasets. As shown in the table, ConfExplainer achieves comparable efficiency to PGExplainer and is significantly faster than ensemble-based methods.

E.1 Ablation Study

To assess the contribution of each component in our proposed approach, we perform an ablation study by decomposing the model into two key variants:

- **w/o Confidence Module:** In this variant, we remove the confidence evaluation module, effectively downgrading our model to a general explainer without confidence assessment.
- **w/o Confidence Loss:** Here, we retain the confidence evaluation module but eliminate the confidence loss, optimizing the module jointly with the Graph Information Bottleneck (GIB) framework.

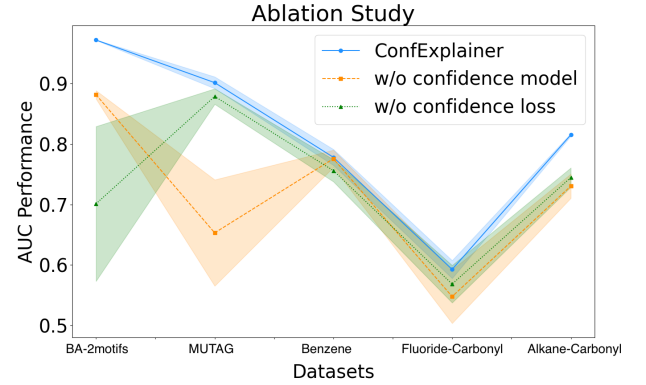


Figure 6: Visualization of ablation study

The results, as shown in Figure 6, demonstrate the effectiveness of our module design. Specifically, the confidence module plays a crucial role in enhancing explanation reliability, while the inclusion of confidence loss further refines the confidence calibration. Notably, our approach maintains comparable performance to the baseline explainer while benefiting from the additional confidence evaluation, validating the necessity of both components.

F Hyper-parameter Tuning

To justify the choice of the confidence loss weight λ , a sensitivity analysis across multiple datasets was conducted by varying λ in $[0.001, 0.01, 0.1, 1, 10, 100, 1000]$. The results of AUC, reported in Table 5, show that ConfExplainer is robust across a wide range of λ values. We chose $\lambda = 100$ as it provides consistently strong performance across datasets.

G Figures

G.1 Visualization of the confidence and explanations over datasets

This section provides additional visualizations of ConfExplainer on different datasets. Figure (7) includes examples from three datasets: (a) Benzene dataset, (b) Fluoride-Carbonyl dataset, and (c) Alkane-Carbonyl dataset.

Each dataset contains two examples. As observed, when ConfExplainer produces accurate explanations, the confidence score is higher. Conversely, for cases where the explanation is not entirely correct, the confidence score is lower. This demonstrates the ability of the confidence module to provide a more reliable assessment of the accuracy of generated explanations.

Received 10 February 2025; accepted 16 May 2025

Dataset	PGE	PGEBE	PGEDE	ConfExplainer
BA-2motifs	283.11	1081.05	1342.88	534.23
MUTAG	2598.70	8532.29	12122.73	4239.88
Benzene	3274.48	12425.79	15630.53	7043.03
Fluoride-Carbonyl	2394.31	9056.82	11324.38	5034.04
Alkane-Carbonyl	311.45	1136.57	1407.92	637.18

Table 4: Training Time Cost

Dataset	0	0.001	0.01	0.1	1	10	100	1000
BA-2motifs	0.7011	0.8271	0.9717	0.9717	0.9719	0.9719	0.9719	0.9717
MUTAG	0.6226	0.9012	0.9011	0.9012	0.9014	0.9017	0.9014	0.9011
Benzene	0.7560	0.7578	0.7694	0.7691	0.7690	0.7890	0.7780	0.7690
Fluoride-Carbonyl	0.7036	0.7691	0.5959	0.5928	0.5927	0.5927	0.5927	0.5927
Alkane-Carbonyl	0.7768	0.8099	0.8055	0.8059	0.8070	0.8275	0.8152	0.8133

Table 5: Hyper-parameter Tuning

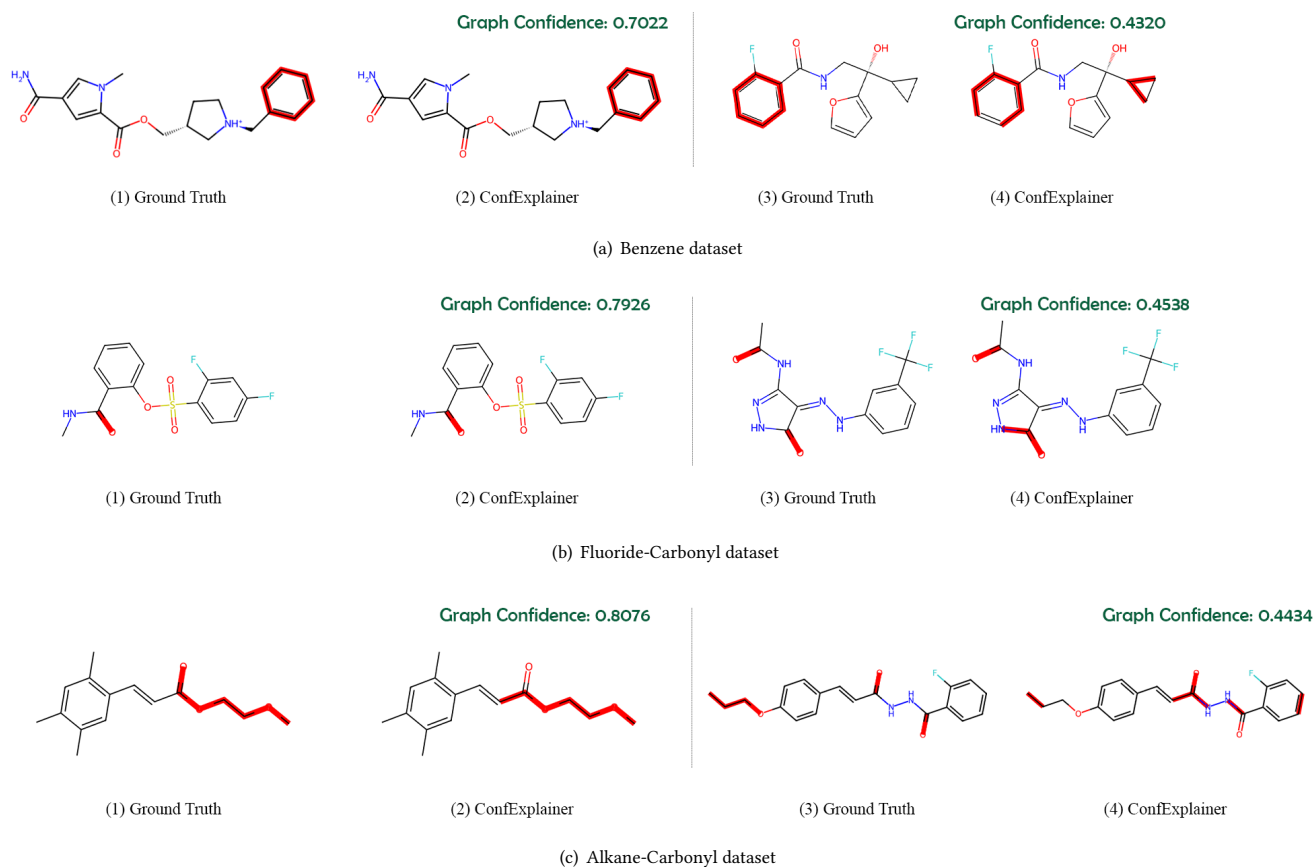


Figure 7: Visualization of additional examples from the Benzene, Fluoride-Carbonyl, and Alkane-Carbonyl datasets, with the highlighted regions indicating the explanations and graph confidence scores.